THE JOURNAL OF PHYSICAL CHEMISTRY C

Article

pubs.acs.org/JPCC

Multiple Reaction Pathways in Shocked 2,4,6-Triamino-1,3,5-trinitrobenzene Crystal

Subodh C. Tiwari, Ken-ichi Nomura, Rajiv K. Kalia, Aiichiro Nakano,* and Priya Vashishta

Collaboratory for Advanced Computing and Simulations, Department of Physics & Astronomy, Department of Computer Science, Department of Chemical Engineering & Materials Science, and Department of Biological Sciences, University of Southern California, Los Angeles, California 90089-0242, United States

Supporting Information

ABSTRACT: Detonation processes probed with atomistic details have remained elusive due to highly complex reactions in heterogeneous shock structures. Here, we provide atomistic details of the initial reaction pathways during shock-induced decomposition of 2,4,6-triamino-1,3,5-trinitrobenzene (TATB) crystal using large reactive molecular dynamics simulations based on reactive force fields. Simulation results reveal the existence of three competing intermolecular pathways for the formation of N_2. We also observe the formation of large nitrogen- and oxygen-rich carbon aggregates, which delays the release of final reaction products.

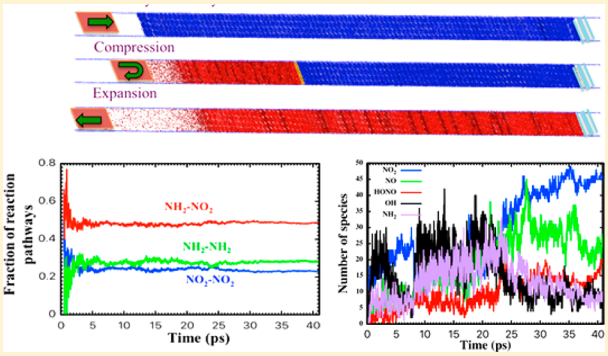

INTRODUCTION

Many organic high-explosive (HE) materials are metastable molecular solids composed of C, H, N, and O atoms. During detonation, HE materials produce stable small molecules such as N_2, H_2O, and CO_2 via complex chemical reactions and release excess energy.[1] The time scale of these detonation processes varies widely from nanoseconds to microseconds, depending on the molecular composition and physical properties (e.g., density and crystal structure) of HEs as well as chemical reaction pathways involved in the decomposition processes.[2,3] However, these processes are very difficult to understand with atomistic detail.[1,4−6]

2,4,6-Triamino-1,3,5-trinitrobenzene (TATB with chemical composition $C_6H_6O_6N_6$, shown in Figure 1a and 1b) is an extremely insensitive yet moderately powerful polyamino-polynitro arene HE material.[7] Its unusual thermal and shock resistances, as well as its chemical stability, make TATB highly important technologically.[8] Due to the interplay of covalent bonds with hydrogen bonds and van der Waals interactions, reactivity of TATB under shock is also a fundamental scientific problem.[7,9−15] Understanding its chemical reaction during the detonation process with atomistic detail may provide insight about the chemical stability of TATB and eventually leads to the discovery of safer and more powerful HE materials. Thus, both the thermal and the shock stability of TATB have been studied in great detail by both experiment and theory.[2,16−20]

In a TATB molecule, the C−NO_2 bond dissociation energy is much lower than the C−NH_2 bond energy.[20] Thus, loss of nitro groups via various possible mechanisms was suggested as a primary pathway. Sharma et al. observed the loss of NO_2 via scission of C−NO_2 bonds as the primary pathway during thermal and photoinduced decomposition.[17] Shock and impact studies by Sharma et al. suggested the formation of benzofurazan or benzofuroxan intermediates.[21] First-principles electronic structure calculations by Wu et al. suggested that intramolecular hydrogen bonding plays a crucial role in the thermal decomposition of TATB.[20] Hydrogen-transfer-mediated ring closure leads to the formation of benzofurazan or benzofuroxan intermediates.[20] Simultaneous thermogravimetric-modulated beam mass spectrometry and time-of-flight velocity spectra measurements also observed the formation of benzofurazan derivatives.[22]

In contrast to these studies, other spectroscopic and thermal studies by Makashir and Kurian suggested C−NH_2 scission as the primary reaction step.[19] Farber and Srivastava suggested a carbon-ring cleavage mechanism for the thermal decomposition of TATB.[16] Another study using time-of-flight mass spectroscopy by Östmark suggested the formation of nitroso compounds in subdetonation of TATB.[18] On the contrary, reactive force field simulation for the thermal decomposition of TATB suggested the presence of more than one mechanism.[23]

Shock decomposition pathways of crystalline TATB were studied by Manna et al. using molecular dynamics (MD) simulations based on the density functional tight binding (SCC-DFTB) method, which also confirmed the presence of nitrogen-rich mono- and dibenzofurazans heterocycles.[2] Heterocyclic clusters formed during the reaction are dynamically stable and eventually form N_2 and CO_2 (or CO). Time scales

Received: May 30, 2017
Revised: July 6, 2017
Published: July 7, 2017

DOI: 10.1021/acs.jpcc.7b05253
J. Phys. Chem. C 2017, 121, 16029−16034

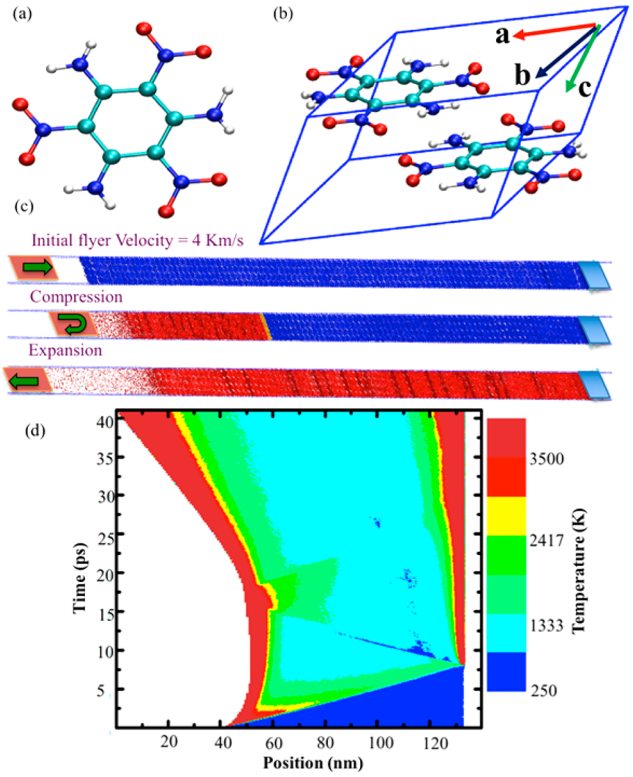

Figure 1. (a) Single TATB molecule where cyan, gray, red, and blue represent carbon, hydrogen, oxygen, and nitrogen, respectively. (b) TATB crystalline unit cell. Each unit cell consists of 2 TATB molecules. Unit cell has lattice parameters of a = 9.010 Å, b = 9.028 Å, c = 6.812 Å, α = 108.58°, β = 91.82°, and γ = 119.97°.[24] (c) Schematic diagram of the system setup. Orange-colored block at the left end of the system represents a repulsive flyer, while the right end is held by a reflective wall. (d) Temperature profile of the system as a function of the position along the a axis and time.

for the formation of these final compounds are in subnanosecond due to the formation of these heterocyclic compounds. These clusters act as reactivity retardants, leading to the shock insensitivity of TATB. However, the formation of these heterocyclic clusters under shock and impact is not well understood, especially within complex heterogeneous shock structures.

Such complex reactions in realistic shock structures can now be studied by large-scale reactive molecular dynamics (RMD) simulations based on first-principles-derived reactive force fields (ReaxFF).[25] We use ReaxFF-lg, ReaxFF with dispersion correction. ReaxFF-lg has been tested for several HEM such as RDX, PETN, and TATB. ReaxFF-lg provides a relatively better equation of state of TATB than ReaxFF. ReaxFF-lg also provides a better ground state description (such as heat of sublimation, density, and cell parameters).[26−28] We study shock-induced decomposition of TATB with atomistic detail. Simulation results provide understanding about the controversial C−NH_2 and C−NO_2 bond scissions as well as the formation of N_2. We identified intermolecular pathways for the formation of N_2 and H_2O. We also observed the formation of a large carbon cluster with high nitrogen and oxygen contents.

COMPUTATIONAL DETAILS

The initial system, shown in Figure 1c, is composed of 100 × 4 × 6 TATB crystalline unit cells (Figure 1b) in a triclinic MD simulation box of dimensions 139.4 nm × 3.568 nm × 3.870 nm along the a, b, and c crystallographic axes. In addition, the MD box includes an empty space of 43 nm at the left end in the a direction in order to observe the evolution of the system over time. In our simulation cell, we applied a 6.3 nm thick reflective wall at the right end. The total number of TATB molecules is 4800, amounting to 115 200 atoms.

The atomic configuration is first relaxed for 6 ps in the canonical (NVT) ensemble at a temperature of 300 K. After thermalization, we introduce a repulsive flyer at the left end of the system with an initial velocity of 4 km/s for shock loading. The repulsive flyer and the reflective wall are at the left and right ends of the system, respectively, as shown in Figure 1c. The interaction between the flyer and the TATB molecules is purely repulsive.

RESULTS AND DISCUSSION

At time t = 0, the flyer starts to move toward the TATB crystal and compresses it, while the repulsion between the flyer and TATB decelerates the flyer. After compression for 10 ps, the repulsive flyer starts to retreat. In the compressed TATB crystal, high temperature and pressure trigger exothermic reactions via chemical decomposition. A supersonic detonation wave from decomposition of TATB travels through the crystal with a speed of 9.98 ± 0.5 km/s. A shock front is clearly identified as a discontinuity in temperature and pressure profiles as shown in Figure S1 in the Supporting Information.[29] Earlier calculation by Manna et al. suggests that hotspot chemistry initiate between 8 and 9 km/s.[2] Reaction products jet out toward left as shown in Figure 1c. Figure 1d shows the temperature profile as a function of the position along the a axis and time. As the flyer hits the TATB crystal, the temperature rises rapidly and a shock wave travels through the TATB crystal. The sharp interface between the unreacted (colored blue) and fully/partially reacted (green/red) regions signifies a shock wave passing through the system. The shock wave reaches the end of the system in ∼10 ps, and the right end of the system starts to heat up due to a rarefaction wave. The fully reacted system expands toward the left empty space as shown by the leftmost red region in Figure 1d.

To study chemical reaction pathways, we perform a fragment analysis. A bond is defined by a unique cutoff value of bond order for each atom pair.[26] A cluster of atoms, connected with covalent bonds, constitutes a molecule. Figure 2 shows the number of molecular products formed as a function of time. Final products include N_2, H_2O, CO_2, and C as shown in eq 1[30]

$$C_6H_6N_6O_6 \rightarrow 3H_2O + 3N_2 + \frac{3}{2}CO_2 + \frac{9}{2}C \quad (1)$$

H_2O is the first product to form. After that we observe the rapid production of both N_2 and H_2O. Unlike in similar HEs such as RDX and HMX, CO_2 is the dominant product compared to CO.[3,23] We observe NH_3 formation at the initial phase. However, the number of NH_3 fragments remains nearly constant after the initial transient. Therefore, NH_3 was not included as part of the final products. Similar behavior was observed during the thermal decomposition of TATB by Quenneville et al.[30]

The time constant for the formation of a product can be estimated by fitting the corresponding number of molecular fragments in Figure 2 to an exponential form as a function of time by using balanced reaction formulas

DOI: 10.1021/acs.jpcc.7b05253
J. Phys. Chem. C 2017, 121, 16029−16034

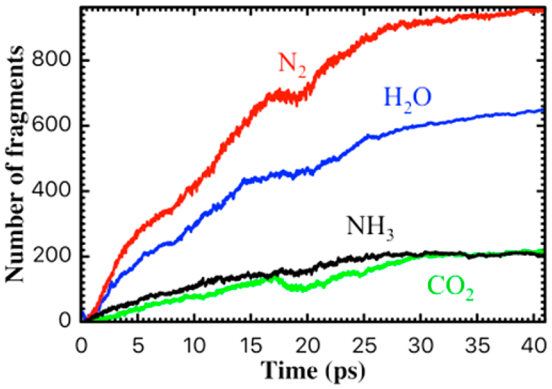

Figure 2. Number of molecular fragments formed as a function of time for shock speed 9.98 km/s. Red, blue, black, and green curves correspond to the formation of N_2, H_2O, NH_3, and CO_2, respectively.

$$n_i(t) = n_{i\infty}\left[1 - \exp\left(-\frac{t}{\tau}\right)\right] \quad (2)$$

Here, $n_i(t)$ is the number of the ith molecular product at time t, $n_{i\infty}$ is the total number of products formed asymptotically ($t \rightarrow \infty$), and τ is the time constant. Least-square fitting provides τ_{H_2O} = 750 ± 200 ps, τ_{N_2} = 500 ± 100 ps, and τ_{CO_2} = 1200 ± 500 ps. A similar time scale was suggested by Manna et al.[2] These results suggest a single-stage reaction for TATB shock decomposition unlike for RDX. Previous studies by Li et al. for RDX shock decomposition found a two-stage reaction, i.e., rapid production of N_2 (τ_{N_2} = 10 ± 2 ps) and H_2O (τ_{H_2O} = 30 ± 4 ps) followed by much slower release of CO_2 (τ_{CO} = 900 ± 400 ps).[3] Shock-induced TATB decomposition does not exhibit any separation of reaction time in the decomposition stage as observed in RDX. Product formation in TATB is also much slower compared to that in RDX, which is consistent with TATB being very insensitive. This correlation between slow product formation and insensitivity in TATB has been discussed in previous literature, where slow decomposition was attributed to the formation of nitrogen-rich heterocyclic compounds. These heterocyclic compounds persist even at very high temperature (3500 K).[2]

To understand the reaction mechanisms for the formation of the final products, we trace back the origin of constituent atoms of N_2 and H_2O molecules. Figure S2 shows the fraction of N_2 and H_2O formed from intramolecular (one molecule) and intermolecular (more than one molecule) reaction pathways.[27] The analysis suggests that intermolecular reaction pathways are dominant for TATB shock decomposition. Approximately 99% of the products are formed via the intermolecular pathways. Similar pathways for the formation of H_2O and N_2 were suggested by Manna et al.[2] Intermolecular pathways seem to be unique for TATB. Similar studies on RDX suggested that 75% of N_2 are formed by intramolecular pathways, i.e., N_2 is formed from a single RDX molecule. Such a pathway exists in RDX due to the presence of $N-NO_2$ bonds within a RDX molecule, which is absent in a TATB molecule.

Intermediate species analysis can provide further insight into the reaction mechanisms. Figure S3 shows the number of intermediate fragments as a function of time.[27] We observe the presence of NO_2 and NH_2 fragments, which can form from the scission of $C-NO_2$ and $C-NH_2$ bonds, respectively. The presence of HONO and NO_2 fragments suggests the formation of N_2 from $C-NO_2$ bond scission. Similar fragments were also observed during the thermal decomposition of nitromethane.[31] This pathway has been suggested for the formation of N_2 in RDX and HMX.[3,32,33] NH_2 from $C-NH_2$ bond scission can form ammonia as the final product by abstracting another hydrogen from N−H bond or form N_2 by recombination with other NH_2 or NO_2 groups. Experimental studies of high-temperature thermal decomposition of TATB show the formation of NH_2.

To further understand the mechanism behind the formation of N_2, we trace back the initial environment of constituent N atoms. We count the number of N_2 molecules formed from different possible combinations, i.e., NH_2-NH_2, NO_2-NH_2, and NO_2-NO_2 pairs. These three pairs represent three different intermolecular reaction pathways I, II, and III, respectively. Table 1 shows the percentage of N_2 molecules that are formed from different reaction pathways after 40 ps. Surprisingly, we observe that 50% of N_2 is formed from NO_2-NH_2 pairs during shock decomposition. The high percentage of N_2 formation from NO_2-NH_2 pairs may be due to the spatial proximity of NH_2 and NO_2 groups in the crystal. In TATB crystal, a NH_2 group from a TATB molecule is adjacent to a NO_2 group from another TATB molecule as shown in Figure S4.[27] As we compress the TATB crystal in the a crystallographic direction, the distance between NH_2 and NO_2 pairs decreases drastically. This may be the reason for reaction pathway II via NO_2-NH_2 being the dominant reaction pathway. Depending on the shock direction in TATB crystal, the reactivity and the primary chemical reaction may change.[14] In HMX and RDX, N_2 products are formed from NO_2-NO_2 pairs. However, N_2 formation from NO_2-NO_2 pair is very low in the case of TATB. While it is clear that NO_2-NH_2 pair dominantly produces N_2 from Table 1, the other reaction pathways cannot be ignored quantitatively, namely, reaction pathways I and III via NH_2-NH_2 and NO_2-NO_2 pairs produce the remaining 50% of N_2.

Table 1. Percentage of N_2 Formed from Different Fragment Pair after 40 ps

fragment pair	% of N_2 formed
NH_2-NH_2	28
NO_2-NH_2	50
NO_2-NO_2	22

In fact, the first step in the shock decomposition of TATB crystal is compressive formation of large clusters from the coalescence of multiple TATB molecules. During the coalescence process, H_2O molecules are released. Due to the extreme compression, we observe the distortion of the planar benzene rings in all three pathways. Detailed analyses suggest that reaction pathways diverge to different reaction pathways to form N_2 from different fragment pairs as shown in the Supporting Information videos.[27] The three videos show the formation of N_2 from reaction pathways I, II, and III. (Though TATB molecules are usually in a large cluster, the complete cluster is not shown in the videos for the clarity of presentation.)

Reaction pathway I (from NH_2-NH_2 pair) to form N_2 undergoes transformation via $C-NH_2$ bond scission from two different TATB molecules. After distortion of the planar structure, the $C-NH_2$ bond breaks to form two NH_2 species. Subsequently, the two NH_2 groups are combined to form N_2. $C-NH_2$ bond breaking has been observed experimentally

DOI: 10.1021/acs.jpcc.7b05253
J. Phys. Chem. C 2017, 121, 16029−16034

under high static pressure.[34] During this process, hydrogen is abstracted by OH or other NH_2 species to form H_2O or NH_3, respectively. The dissociation energy for the C−NH_2 bond is very high compared to that of the C−NO_2 bond,[20] but spectroscopic studies suggest that hydrogen bonding with the C−NO_2 group weakens the C−NH_2 bond.[19,35] The presence of NH_3 has been experimentally observed,[36] which suggests the presence of this pathway. Even though it is not a primary reaction pathway, it accounts for 28% of the production of N_2.

Reaction pathway II (from NH_2−NO_2 pair) is found to be the primary channel for the production of N_2, accounting for 50% of the total N_2 produced. The first step in this channel is the loss of oxygen assisted by an intramolecular/intermolecular NH_2 group. Oxygen loss was also reported experimentally in the decomposition of TATB molecules.[18] NO species react with nearby NH_2 groups from other TATB molecules to form N_2 and H_2O/OH. Hydrogen and oxygen are abstracted by OH and NH_2 species to form water and ammonia. This reaction pathway was also observed in quantum molecular dynamics studies performed by He et al.[37]

Reaction pathway III (from NO_2−NO_2 pair) contributes only 22% in the formation of N_2. This reaction starts with the breaking of the C−NO_2 bond from two nearby TATB molecules. We also observe the presence of NO_2 as an intermediate in shock decomposition of TATB. Two NO_2 species form N_2 as a final product. C−NO_2 bond breaking has been observed experimentally under high static pressure.[34]

To understand the timeline of these reactions, Figure 3 shows the fraction of N_2 formed from different reaction

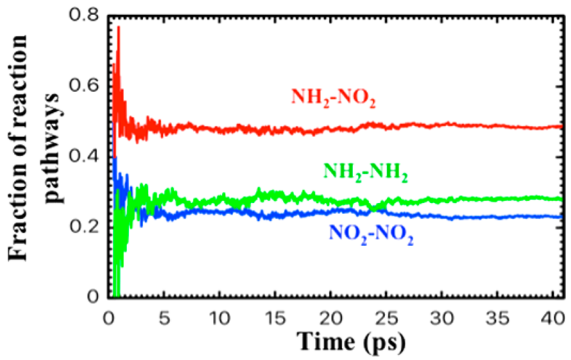

Figure 3. Time evolution of the fraction of N_2 formed from different reaction pathways.

pathways as a function of time. The figure shows that the NH_2−NO_2 pathway (reaction pathway II) dominates over the other two pathways (reaction pathways I and III). Reaction pathway III dominates over reaction pathway I in the early stage of the reaction, since the C−NO_2 bond energy is lower than the C−NH_2 bond energy. Thus, N_2 formation via reaction pathway III is higher. However, after 3 ps, reaction pathway I become the most favorable reaction pathway. Experimental studies of photoinduced decomposition of TATB at ambient and high pressures by Glascoe et al. suggest that elevated pressure may inhibit the hemolysis of the C−NO_2 bond and block the primary decomposition process.[38]

Finally, we perform the stoichiometric analysis for the large clusters. Figure 4a shows the fraction of the number of atoms in large clusters with respect to the total number of atoms. Here, a large cluster is defined as a cluster that contains more than 24 atoms. The number of large clusters increases rapidly first as the

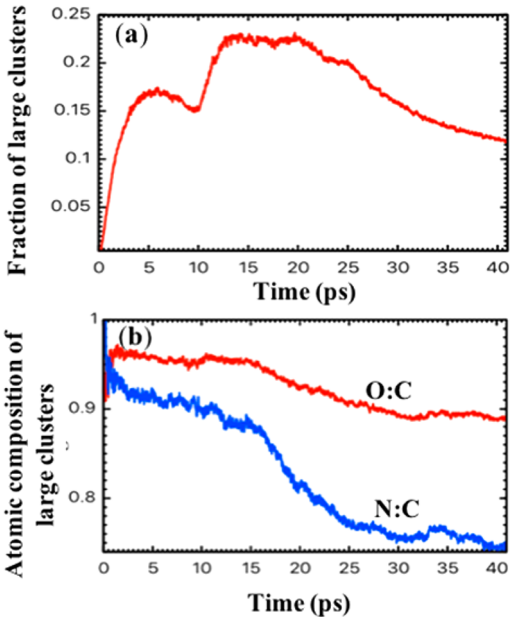

Figure 4. Time evolution of large clusters (number of atoms in the cluster, $n > 24$). (a) Fraction of the number of atoms in large clusters to the total number of atoms. (b) Atomic composition of the large clusters as a function of time. Red and blue lines correspond to the O:C and N:C ratios, respectively.

flyer starts to compress TATB crystal. When the rarefaction wave returns, the fraction of large clusters increase again. After 20 ps, the number of large cluster starts to decline.

Figure 4b shows the carbon-to-oxygen (red line) and carbon-to-nitrogen (blue line) ratios in the large clusters. We observe that large clusters are nitrogen and oxygen rich, which delay the formation of stable products such as N_2, CO_2, and H_2O in later stages. Most of the final products seep out of these large clusters. Quantum molecular dynamics studies by Manna et al. found the presence of nitrogen-rich clusters, which impede the formation of N_2.[2] Oxygen-rich clusters were also reported in shock simulation of RDX[3] and thermal decomposition of TATB.[23]

CONCLUSION

In summary, our RMD simulations reveal that N_2 production in shock decomposition of TATB is a multichannel process. Reaction mechanism studies suggest that a reaction pathway via NH_2−NO_2 pairs is the primary reaction pathway for the formation of N_2. However, other two pathways (from NH_2−NH_2 and NO_2−NO_2 pairs) also participate significantly in the formation of N_2. Primary reaction stages include the formation of N_2 and H_2O rapidly and then somewhat slower formation of CO_2. Most of the products formed via intermolecular pathways.

ASSOCIATED CONTENT

Supporting Information

The Supporting Information is available free of charge on the ACS Publications website at DOI: 10.1021/acs.jpcc.7b05253.

Intermediate analysis and shock speed analysis (PDF)

Movie for formation of N_2 from reaction pathway I (AVI)

Movie for formation of N_2 from reaction pathway II (AVI)

DOI: 10.1021/acs.jpcc.7b05253
J. Phys. Chem. C 2017, 121, 16029−16034

Movie for formation of N_2 from reaction pathway III (AVI)

AUTHOR INFORMATION

Corresponding Author

*E-mail: anakano@usc.edu.

ORCID

Aiichiro Nakano: 0000-0003-3228-3896

Notes

The authors declare no competing financial interest.

ACKNOWLEDGMENTS

This work was supported by the Air Force Office of Scientific Research Grant No. FA9550-16-1-0042.

REFERENCES

(1) Bastea, S.; Fried, L. E. *Shock Waves Science and Technology Library*; Springer Berlin Heidelberg: Berlin, Heidelberg, 2012; Vol. *6* (Detonation Dynamics), pp 1−31.

(2) Manaa, M. R.; Reed, E. J.; Fried, L. E.; Goldman, N. Nitrogen-Rich Heterocycles as Reactivity Retardants in Shocked Insensitive Explosives. *J. Am. Chem. Soc.* **2009**, *131*, 5483−5487.

(3) Li, Y.; Kalia, R. K.; Nakano, A.; Nomura, K.; Vashishta, P. Multistage Reaction Pathways in Detonating High Explosives. *Appl. Phys. Lett.* **2014**, *105*, 204103.

(4) Dlott, D. D.; Fayer, M. D. Shocked Molecular-Solids - Vibrational up Pumping, Defect Hot Spot Formation, and the Onset of Chemistry. *J. Chem. Phys.* **1990**, *92*, 3798−3812.

(5) White, C. T.; Sinnott, S. B.; Mintmire, J. W.; Brenner, D. W.; Robertson, D. H. Chemistry and Phase Transitions from Hypervelocity Impacts. *Int. J. Quantum Chem.* **1994**, *52*, 129−137.

(6) Wu, C. J.; Fried, L. E.; Yang, L. H.; Goldman, N.; Bastea, S. Catalytic Behaviour of Dense Hot Water. *Nat. Chem.* **2009**, *1*, 57−62.

(7) Zeman, S. Thermal Stabilities of Polynitroaromatic Compounds and Their Derivatives. *Thermochim. Acta* **1979**, *31*, 269−283.

(8) Dobratz, B. M. *The Insensitive High Explosive Triaminotrinitrobenzene (TATB): Development and Characterization−1888 to 1994*; Los Alamos National Laboratory, 1994.

(9) Brenner, D. W.; Robertson, D. H.; Elert, M. L.; White, C. T. Detonations at Nanometer Resolution Using Molecular Dynamics. *Phys. Rev. Lett.* **1993**, *70*, 2174−2177.

(10) Kennedy, J. E.; Lee, K.-Y.; Son, S. F.; Martin, E. S.; Asay, B. W.; Skidmore, C. B. Second-Harmonic Generation and the Shock Sensitivity of TATB. *AIP Conf. Proc.* **1999**, *505*, 711−714.

(11) Riad Manaa, M. Shear-Induced Metallization of Triamino-Trinitrobenzene Crystals. *Appl. Phys. Lett.* **2003**, *83*, 1352−1354.

(12) Elert, M. L.; Zybin, S. V.; White, C. T. Molecular Dynamics Study of Shock-Induced Chemistry in Small Condensed-Phase Hydrocarbons. *J. Chem. Phys.* **2003**, *118*, 9795−9801.

(13) Davidson, A. J.; Dias, R. P.; Dattelbaum, D. M.; Yoo, C. S. Stubborn" Triaminotrinitrobenzene: Unusually High Chemical Stability of a Molecular Solid to 150 GPa. *J. Chem. Phys.* **2011**, *135*, 174507.

(14) Shimamura, K.; Misawa, M.; Li, Y.; Kalia, R. K.; Nakano, A.; Shimojo, F.; Vashishta, P. A Crossover in Anisotropic Nanomechanochemistry of Van Der Waals Crystals. *Appl. Phys. Lett.* **2015**, *107*, 231903.

(15) Li, Y.; Kalia, R. K.; Misawa, M.; Nakano, A.; Nomura, K.; Shimamura, K.; Shimojo, F.; Vashishta, P. Anisotropic Mechanoresponse of Energetic Crystallites: A Quantum Molecular Dynamics Study of Nano-Collision. *Nanoscale* **2016**, *8*, 9714−9720.

(16) Farber, M.; Srivastava, R. D. Thermal Decomposition of 1,3,5-Triamino-2,4,6-Trinitrobenzene. *Combust. Flame* **1981**, *42*, 165−171.

(17) Sharma, J.; Garrett, W. L.; Owens, F. J.; Vogel, V. L. X-Ray Photoelectron Study of Electronic Structure, Ultraviolet, and Isothermal Decomposition of 1,3,5-Triamino-2,4,6-Trinitrobenzene. *J. Phys. Chem.* **1982**, *86*, 1657−1661.

(18) Östmark, H. Shock Induced Sub-Detonation Chemical Reactions in 1,3,5-Triamino-2,4,6-Trinitrobenzene. *AIP Conf. Proc.* **1995**, *370*, 871−874.

(19) Makashir, P. S.; Kurian, E. M. Spectroscopic and Thermal Studies on the Decomposition of 1,3,5-Triamino-2,4,6-Trinitrobenzene (TATB). *J. Therm. Anal.* **1996**, *46*, 225−236.

(20) Wu, C. J.; Fried, L. E. Ring Closure Mediated by Intramolecular Hydrogen Transfer in the Decomposition of a Push−Pull Nitroaromatic: TATB. *J. Phys. Chem. A* **2000**, *104*, 6447−6452.

(21) Sharma, J.; Forbes, J. W.; Coffey, C. S.; Liddiard, T. P. The Physical and Chemical Nature of Sensitization Centers Left from Hot Spots Caused in Triaminotrinitrobenzene by Shock or Impact. *J. Phys. Chem.* **1987**, *91*, 5139−5144.

(22) Land, T. A.; Siekhaus, W. J.; Foltz, M. F.; Behrens, R. J. Condensed-Phase Thermal Decomposition of Tatb Investigated by Atomic Force Microscopy (AFM) and Simultaneous Thermogravimetric Modulated Beam Mass Spectrometry (STMBMS). In *Conference: 10. detonation symposium*, Boston, MA, July 12−16, 1993; Other Information: PBD: May 1993; Lawrence Livermore National Laboratory, 1993; p 10.

(23) Zhang, L.; Zybin, S. V.; van Duin, A. C. T.; Dasgupta, S.; Goddard, W. A.; Kober, E. M. Carbon Cluster Formation During Thermal Decomposition of Octahydro-1,3,5,7-Tetranitro-1,3,5,7-Tetrazocine and 1,3,5-Triamino-2,4,6-Trinitrobenzene High Explosives from Reaxff Reactive Molecular Dynamics Simulations. *J. Phys. Chem. A* **2009**, *113*, 10619−10640.

(24) Cady, H. H.; Larson, A. C. The Crystal Structure of 1,3,5-Triamino-2,4,6-Trinitrobenzene. *Acta Crystallogr.* **1965**, *18*, 485−496.

(25) Nomura, K.; Small, P. E.; Kalia, R. K.; Nakano, A.; Vashishta, P. An Extended-Lagrangian Scheme for Charge Equilibration in Reactive Molecular Dynamics Simulations. *Comput. Phys. Commun.* **2015**, *192*, 91−96.

(26) Liu, L.; Liu, Y.; Zybin, S. V.; Sun, H.; Goddard, W. A. Reaxff-Lg: Correction of the Reaxff Reactive Force Field for London Dispersion, with Applications to the Equations of State for Energetic Materials. *J. Phys. Chem. A* **2011**, *115*, 11016−11022.

(27) Rice, B. M.; Larentzos, J. P.; Byrd, E. F. C.; Weingarten, N. S. Parameterizing Complex Reactive Force Fields Using Multiple Objective Evolutionary Strategies (Moes): Part 2: Transferability of Reaxff Models to C−H−N−O Energetic Materials. *J. Chem. Theory Comput.* **2015**, *11*, 392−405.

(28) Zhou, T.; Song, H.; Liu, Y.; Huang, F. Shock Initiated Thermal and Chemical Responses of HMX Crystal from Reaxff Molecular Dynamics Simulation. *Phys. Chem. Chem. Phys.* **2014**, *16*, 13914−13931.

(29) See Supporting Information for simulation methods and details.

(30) Quenneville, J.; Germann, T. C.; Thompson, A. P.; Kober, E. M. Molecular Dynamics Studies of Thermal Induced Chemistry in Tatb. *AIP Conf. Proc.* **2007**, *955*, 451−454.

(31) Chang, J.; Lian, P.; Wei, D.-Q.; Chen, X.-R.; Zhang, Q.-M.; Gong, Z.-Z. Thermal Decomposition of the Solid Phase of Nitromethane: Ab Initio Molecular Dynamics Simulations. *Phys. Rev. Lett.* **2010**, *105*, 188302.

(32) Ge, N.-N.; Wei, Y.-K.; Ji, G.-F.; Chen, X.-R.; Zhao, F.; Wei, D.-Q. Initial Decomposition of the Condensed-Phase β-Hmx under Shock Waves: Molecular Dynamics Simulations. *J. Phys. Chem. B* **2012**, *116*, 13696−13704.

(33) Schweigert, I. V. Ab Initio Molecular Dynamics of High-Temperature Unimolecular Dissociation of Gas-Phase RDX and Its Dissociation Products. *J. Phys. Chem. A* **2015**, *119*, 2747−2759.

(34) Crowhurst, J. C.; Stavrou, S.; Zaug, J. M.; Armstrong, M. R.; Radousky, H. B.; Fried, L. E. Decomposition Products of TATB under High Static Pressure, In *Conference: APS March Meeting 2016*, Baltimore, Baltimore, 2016.

(35) Britt, A. D.; Moniz, W. B.; Chingas, G. C.; Moore, D. W.; Heller, C. A.; Ko, C. L. Free Radicales of TATB. *Propellants, Explos., Pyrotech.* **1981**, *6*, 94−95.

DOI: 10.1021/acs.jpcc.7b05253
J. Phys. Chem. C 2017, 121, 16029−16034

(36) Ornellas, D. L. *Calorimetric Determinations of the Heat and Products of Detonation for Explosives: October 1961 to April 1982*; Lawrence Livermore National Laboratory, 1982.
(37) He, Z.-H.; Chen, J.; Wu, Q. Initial Decomposition of Condensed-Phase 1,3,5-Triamino-2,4,6-Trinitrobenzene under Shock Loading. *J. Phys. Chem. C* **2017**, *121*, 8227−8235.
(38) Glascoe, E. A.; Zaug, J. M.; Armstrong, M. R.; Crowhurst, J. C.; Grant, C. D.; Fried, L. E. Nanosecond Time-Resolved and Steady-State Infrared Studies of Photoinduced Decomposition of TATB at Ambient and Elevated Pressure. *J. Phys. Chem. A* **2009**, *113*, 5881−5887.

DOI: 10.1021/acs.jpcc.7b05253
J. Phys. Chem. C 2017, 121, 16029−16034